Waveform-controlled near-single-cycle milli-joule laser pulses generate sub-10 nm extreme ultraviolet continua

Wolfgang Schweinberger,[1,4] Annkatrin Sommer,[1] Elisabeth Bothschafter,[1,3] Jiang Li,[1] Ferenc Krausz,[1,2] Reinhard Kienberger,[1,3] and Martin Schultze[1,2,*]

[1]*Max-Planck-Institut für Quantenoptik, Hans-Kopfermann-Strasse 1, D-85748 Garching, Germany*

[2]*Department für Physik, Ludwig Maximilians Universität, Am Coulombwall 1, D-85748 Garching, Germany*

[3]*Physik-Department, Technische Universität München, James-Franck-Strasse 1, D-85748 Garching, Germany*

[4]*e-mail: wolfgang.schweinberger@mpq.mpg.de*

**Corresponding author: martin.schultze@mpq.mpg.de*

Received April 19, 2012; revised June 29, 2012; accepted July 2, 2012;
posted July 5, 2012 (Doc. ID 167042); published August 23, 2012

We demonstrate the generation of waveform-controlled laser pulses with 1 mJ pulse energy and a full-width-half-maximum duration of ~4 fs, therefore lasting less than two cycles of the electric field oscillating at their carrier frequency. The laser source is carrier-envelope-phase stabilized and used as the backbone of a kHz repetition rate source of high-harmonic continua with unprecedented flux at photon energies between 100 and 200 eV (corresponding to a wavelength range between 12–6 nm respectively). In combination we use these tools for the complete temporal characterization of the laser pulses via attosecond streaking spectroscopy.

OCIS codes: 140.7090, 320.5520, 320.7110.

The power of attosecond metrology is continuously driven by achievements made in the field of ultrashort laser pulses. The first experiments with a temporal resolution truly beyond the femtosecond limit [1] became feasible right after the demonstration of sub-5 fs laser pulses. These turned out to be a precondition for the direct synthesis of isolated extreme ultraviolet (XUV) attosecond pulses in the high-harmonic generation (HHG) scheme. This scheme describes the generation of attosecond pulses in the recollision [2,3] picture in which the linearly polarized field of an intense laser pulse causes tunnel ionization of a noble gas atom. The electron that is released to the vacuum is then accelerated by the strong electric laser field and might finally reunite with its parent ion after the field changed sign half a cycle later. The kinetic energy the electron collected during acceleration, plus its binding energy, is released as a burst of XUV radiation that, properly filtered, forms a pulse isolated in time. Since the first demonstration of isolated attosecond pulses, the driving laser pulses became ever shorter, approaching the single cycle limit [4]. Further sequential reduction of the duration of the attosecond pulses permitted more and more elaborate attosecond studies with demonstrated pulse durations below 100 attoseconds [5,6]. While the duration of attosecond pulses is affected by the duration of the driving laser fields, the range of photon energies (and the photon flux) accessible to attosecond spectroscopy depends critically on the energy content of each laser pulse.

Here we introduce an ultrafast laser source capable of generating near-single-cycle-mJ-pulses and demonstrate how these pulses extend the scope of attosecond technology to photon energies of ~200 eV with a flux comparable to HHG attosecond sources at lower energies.

Laser pulses are generated in a mode-locked Ti:Sa oscillator with active carrier-envelope-phase (CEP) stabilization based on the f-to-0 scheme [7]. The difference between the carrier-envelope phase slip frequency f_{CEO} and the laser oscillator's repetition rate f_{OSC} is regulated by control electronics to be constant via feedback to the oscillators pumping power. The pulse energy amounts to 2 nJ within 7 fs full width at half maximum (FWHM) duration.

These pulses are then dispersed by a grating-prism combination (grism) [8] introducing negative dispersion. Subsequently, the pulses are amplified in a 9-pass Ti:Sapphire chirped pulse amplifier (CPA) (Femtopower compact Pro). After the fourth pass a pulse picker reduces the repetition rate to 4 kHz and a *Dazzler* (Fastlite) serves as an antigain-narrowing filter and at the same time corrects residual higher-order phase distortions. We achieve output pulse energies of 1.1 mJ within 65 nm FWHM bandwidth shifted about 8 nm to the blue compared to the classic positive dispersion setup [4,9]. Two position sensors continuously monitor the output beam's position and direction, and a computer controlled feedback loop compensates for drifts by actuating two piezo controlled mirrors at the exit of the laser chain.

A second amplification stage further boosts the output energy. This stage consists of a 6 mm aperture Ti:Sa crystal cryo-cooled down to 70 K and is pumped by two counter-propagating Thales *ETNA HP*. The experiments described here rely on a single additional amplification pass for the 800 nm light and in total 90 W pumping power at 532 nm (22.5 mJ/pulse) resulting in a pulse energy of 2.1 mJ, for a system layout see Fig. 1(a).

Compression is achieved in a bulk glass compressor [Fig. 1(c)] that features only little transmission losses and furthermore is inherently alignment and jitter-free and thus provides reliable CEP stability.

Damage threshold considerations demanded minimal pulse duration of 25 ps in the amplification step, considering the spectral extension of the laser pulses demonstrated here that corresponds to the introduction of

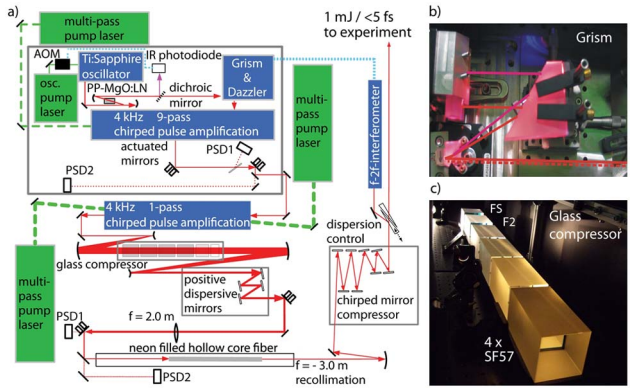

Fig. 1. (Color online) (a) Schematic laser setup with mode-locked Ti:Sa oscillator and two multipass amplification stages. For details see text. Panel (b) shows a photograph of the grism setup with sketched rays. The glass-block compressor [see panel (c)] transmits >85%.

approximately-170000 fs^2, at the central wavelength of 790 nm. The 13×17 cm grism stretcher [Fig. 1(b)] introduces this amount of negative dispersion between the oscillator and the first amplification stage and features a transmission of ~50%.

The grism parameters are chosen to compensate the bulk glass compressor (138000 fs^2, 90000 fs^3) and all the dispersive elements after the oscillator (30000 fs^2, 20000 fs^3). We selected four 13.5 cm long blocks of AR-coated HHTSF57 with 7×7 cm free aperture to achieve quick compression (about 90% of the reduction in pulse duration) down to pulse durations susceptible to B-Integral and achieve the last compression step in 115 mm F2 and 100 mm fused silica [see Fig. 1(c)]. To further reduce the extent of nonlinear effects in the glass-block compressor, the ultimate compression step is achieved via four dielectric mirrors with positive dispersion (300 fs^2 per reflection) that are placed behind the glass blocks to avoid the transmission of the Fourier-limited, i.e. highly intense pulses, through bulk glass.

After the compression with glass blocks and dispersive mirrors, the remaining pulse energy is 1.8 mJ and the pulse duration is 23 fs as measured by second order autocorrelation and frequency-resolved optical gating (FROG). Obviously, this CPA concept shifts the difficulties of proper alignment and the transmission constraints from the end of the laser chain (prims- or grating compressors in conventional CPA systems) to the starting point of the laser chain. The grism [Fig. 1(b)], though not trivial to align in the first setup procedure, due to its small footprint and rigid design, is by far less susceptible to mechanic vibrations (affecting the CEP stability) compared to the square-meter scale prism compressors used in other laser systems. In addition, placing the low-transmission component of the dispersion management before the amplification reduces the overall heat-load deposited in the laser system.

Crucial to all nonlinear or ultrafast experiments is the stability of the CE phase. To ensure a stable waveform of each subsequent laser pulse, the attenuated beam of a reflection is sent to a compact f-to-2f interferometer [10]. A fast Fourier transform (FFT) algorithm assigns a phase to the observed signal and thus provides an error signal. Feedback is applied by moving the first grating and prism in the grism-stretcher with a shear-piezo stack to compensate for phase drifts. The standard deviation of the signal is 42 mrad. The piezo provides a slow loop range of $\pm 6\pi$. This system grants CE-phase stability typically over several hours with fluctuations of the pulse energy of <1.5% root mean square limited by the pump laser stability.

After compression the pulses are focused into a hollow core fiber (HCF), 400 μm inner diameter, length 1.15 m, in a neon filled gas cell. Self-phase modulation broadens their spectrum sufficiently to cover the bandwidth between 500 and 1000 nm that, given proper dispersion management, supports a sub-two-cycle pulse. With 1.1 mJ output energy, the transmission exceeds 60%. Compression of the pulses is achieved by a pair of thin fused silica wedges and a chirped mirror compressor with eight reflections (–35 fs^2 each) using the double angle technique that draws on identical mirrors used at two different angles of incidence. This yields antiphase oscillations of the group delay dispersion (as they are typical for multilayer mirrors) and the resulting spectral phase is flat. Due to their large spectral width, at the very limits of conventional methods to determine the pulse duration, we applied attosecond streaking spectroscopy in neon [5,11,12] to determine a pulse duration of 4.5 fs. The recorded time evolution of the laser pulses is displayed in Fig. 2. Even moderately focused (e.g. focal length $f = 60$ cm), these parameters correspond to intensities above 10^{15} W/cm^2 making this laser system an ideal tool for the generation of high-harmonic radiation.

To explore the potential of this laser source we generated high-harmonic radiation and investigated the emitted spectra. The limiting factor for the intensity of the laser pulses driving the HHG process is the occurrence of irreversible ionization at low intensities. Due to its larger ionization potential, I_p, in comparison to neon, we have thus chosen helium as target medium. At the same time, the larger I_p and higher driving intensities allow the released electrons to accumulate more kinetic energy and in turn to emit higher energetic photons [13].

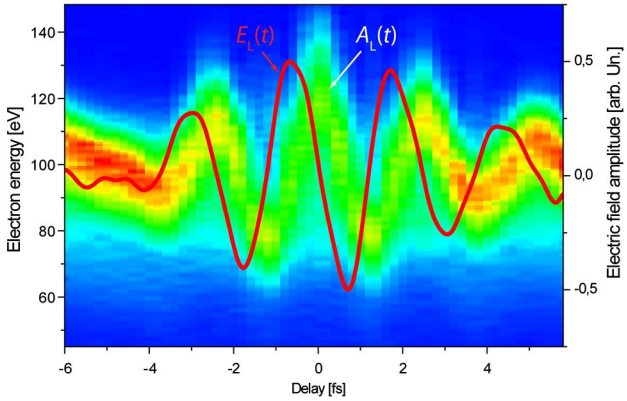

Fig. 2. (Color online) Attosecond streaking spectrogram of the 1 mJ laser pulses. The solid curve $E_L(t)$ is the temporal evolution of the instantaneous laser electric field extracted from the vector potential $A_L(t)$ that streaking spectroscopy measures. The isolated attosecond pulses at 120 eV central photon energy have a duration of 170 as.

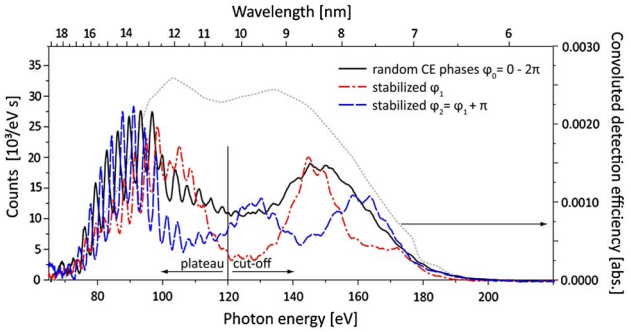

Fig. 3. (Color online) High-harmonic spectra generated in helium. A grazing incidence grating spectrometer is used to spectrally resolve the emitted light bursts; low energetic radiation is suppressed by a 1 μm thick zirconium foil. The black line was recorded with the CE-phase varying randomly while the dashed and the dash-dotted line show the spectra as obtained for two settings of the CE-phase that differ by π. The dotted line indicates the spectral response of the spectrometer. The curve is the superposition of the filter transmittance and the reflectance of one grazing incidence gold mirror (data taken from [14]), the grating efficiency (Hitachi) and the CCD's quantum efficiency (Roper).

Figure 3 summarizes our findings using the same experimental setup that was used to trace the electric field of the laser pulses with attosecond streaking but now with helium at a backing pressure of 160 mbar in the same target geometry and focusing. Clearly the combination of the highly intense laser pulses with helium as nonlinear medium allows attosecond spectroscopy to unfold its potential in new wavelength regions. The spectra show a distinct modulation with periodicity of twice the fundamental photon energy as expected for the plateau region. The occurrence of this modulation is a result of the contribution of more than one recollision event to this spectral range (and it proves the ability of the spectrometer to resolve this 2ω modulation). At the same time we observe a non modulated spectral shape in the cut-off region with distinct influence of the CE-phase setting. This spectral shape, along with the strong dependence on the CE phase of the cut-off region, strongly suggests that in this spectral range, only a single attosecond pulse is emitted. These findings not only offer the potential of expanding the horizon of attosecond spectroscopy to the 100–200 eV photon energy range, but also hold promise for a new record short-XUV pulse duration.

The authors acknowledge technical support from Thales Optronique S. A. This work is supported by the Max Planck Society and the Deutsche Forschungsgemeinschaft Cluster of Excellence: Munich Centre for Advanced Photonics. R. K. acknowledges support from the Sofia Kovalevskaya award of the Alexander von Humboldt Foundation.

References

1. R. Kienberger, M. Hentschel, M. Uiberacker, C. Spielmann, M. Kitzler, A. Scrinzi, M. Wieland, T. Westerwalbesloh, U. Kleineberg, U. Heinzmann, M. Drescher, and F. Krausz, Science **297**, 1144 (2002).
2. P. Corkum, Phys. Rev. Lett. **71**, 1994 (1993).
3. J. Krause, K. Schafer, and K. Kulander, Phys. Rev. A **45**, 4998 (1992).
4. A. L. Cavalieri, E. Goulielmakis, B. Horvath, W. Helml, M. Schultze, M. Fieß, V. Pervak, L. Veisz, V. S. Yakovlev, M. Uiberacker, A. Apolonski, F. Krausz, and R. Kienberger, New J. Phys. **9**, 242 (2007).
5. E. Goulielmakis, M. Schultze, M. Hofstetter, V. S. Yakovlev, J. Gagnon, M. Uiberacker, A. L. Aquila, E. M. Gullikson, D. T. Attwood, R. Kienberger, F. Krausz, and U. Kleineberg, Science **320**, 1614 (2008).
6. G. Sansone, E. Benedetti, F. Calegari, C. Vozzi, L. Avaldi, R. Flammini, L. Poletto, P. Villoresi, C. Altucci, R. Velotta, S. Stagira, S. De Silvestri, and M. Nisoli, Science **314**, 443 (2006).
7. T. Fuji, J. Rauschenberger, A. Apolonski, V. S. Yakovlev, G. Tempea, T. Udem, C. Gohle, T. W. Hänsch, W. Lehnert, M. Scherer, and F. Krausz, Opt. Lett. **30**, 332 (2005).
8. S. Kane and J. Squier, IEEE J. Quantum Electron. **31**, 2052 (1995).
9. X. Chen, A. Jullien, A. Malvache, L. Canova, A. Borot, A. Trisorio, C. G. Durfee, and R. Lopez-Martens, Opt. Lett. **34**, 1588 (2009).
10. M. Schultze, A. Wirth, I. Grguras, M. Uiberacker, T. Uphues, A. J. Verhoef, J. Gagnon, M. Hofstetter, U. Kleineberg, E. Goulielmakis, and F. Krausz, J. Electron Spectrosc. Relat. Phenom. **184**, 68 (2011).
11. Y. Mairesse and F. Quéré, Phys. Rev. A **71**, 011401 (2005).
12. J. Gagnon and V. S. Yakovlev, Opt. Express **17**, 17678 (2009).
13. M. Lewenstein, P. Balcou, M. Ivanov, A. L'Huillier, and P. Corkum, Phys. Rev. A **49**, 2117 (1994).
14. B. L. Henke, E. M. Gullikson, and J. C. Davis, At. Data Nucl. Data Tables **54**, 181 (1993).